The Aerodynamics of Free-Flight Maneuvers in *Drosophila*

Steven N. Fry,[1] Rosalyn Sayaman,[2] Michael H. Dickinson[2]*

Using three-dimensional infrared high-speed video, we captured the wing and body kinematics of free-flying fruit flies as they performed rapid flight maneuvers. We then "replayed" the wing kinematics on a dynamically scaled robotic model to measure the aerodynamic forces produced by the wings. The results show that a fly generates rapid turns with surprisingly subtle modifications in wing motion, which nonetheless generate sufficient torque for the fly to rotate its body through each turn. The magnitude and time course of the torque and body motion during rapid turns indicate that inertia, not friction, dominates the flight dynamics of insects.

Brisk right-angle turns, termed body saccades, are characteristic of many flies (insects of the order Diptera). Saccades are very fast: A fly can change direction by 90° in less than 50 ms (*1*–*3*). To turn, a fly must generate torque to overcome both the inertia of its body and the viscous friction of the air. The relative importance of these forces is largely influenced by body size. Large animals must overcome inertial forces when they accelerate or turn, whereas small animals must overcome the viscous forces acting on their bodies. Current models of flight assume that inertia plays a minor role in the dynamics of

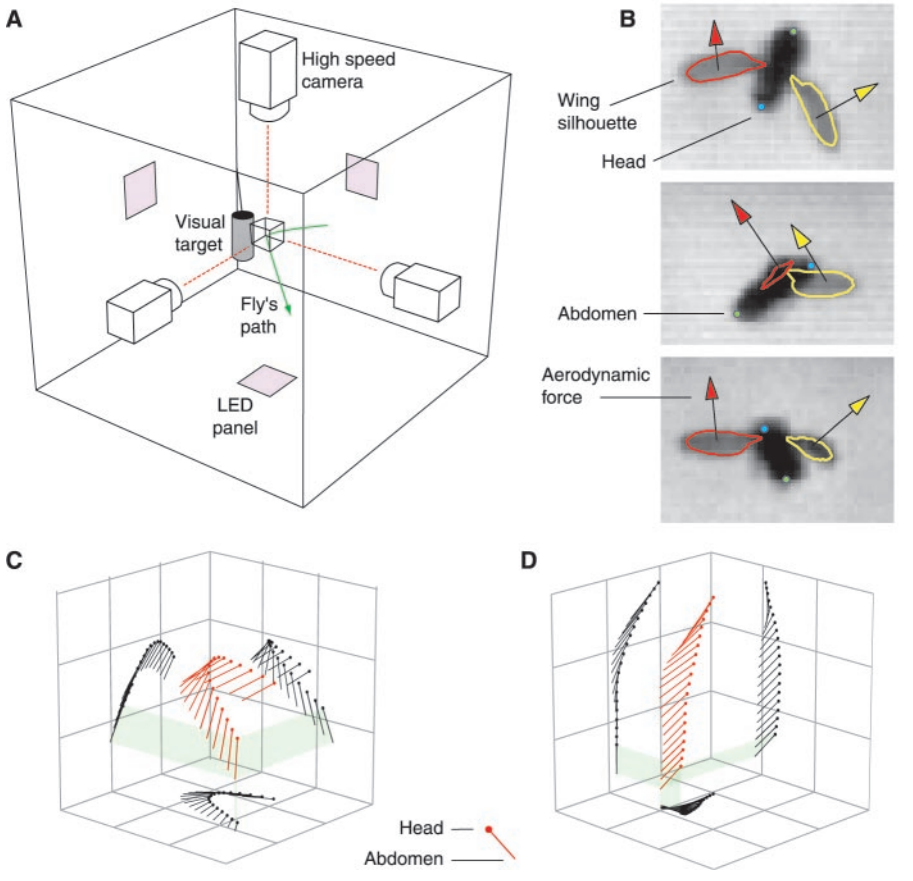

Fig. 1. (**A**) Experimental setup used to film flight maneuvers. Flies were released into an enclosed flight chamber and imaged with three high-speed cameras at 5000 frames per second. (**B**) Corresponding frames from which three-dimensional body and wing positions were extracted. Wing models and measured flight forces are superimposed. (**C** and **D**) Body kinematics during saccadic turning maneuvers. Body orientation for every 25th position of the captured sequence is shown in red, with corresponding orthogonal projections shown in black. In (C), the fly approached the target, performed a saccade, and then accelerated away in a different direction. In (D), the fly performed a saccade during a vertical ascent. Grid width, 5 mm. For details of this and other figures, see (*6*) and movie S1.

the proposed checkpoint mechanism to coordinate transcription and pre-mRNA processing via CTD phosphorylation (*17*) (fig. S8). Furthermore, modulation of the levels (*25*, *26*) or activity (*6*) of these factors might regulate the release of RNAPII into the elongation phase, allowing transcription in yeast to be matched to the environmental conditions and the availability of nutrients. An outstanding question is how, in the absence of high-affinity binding sites and a cooperative binding partner, the Fkh factors associate with chromatin in coding regions. Like Dst1p, the Fkh factors may directly associate with elongating RNAPII (*27*). An alternative possibility is that the Fkh factors are tethered to specific domains of chromatin in coding regions (*28*). It remains to be determined how the diverse activities of Fkh factors in metazoans will relate to this demonstrated role in transcriptional elongation.

References and Notes

1. P. Carlsson, M. Mahlapuu, *Dev. Biol.* **250**, 1 (2002).
2. I. Simon *et al.*, *Cell* **106**, 697 (2001).
3. G. Zhu *et al.*, *Nature* **406**, 90 (2000).
4. M. Koranda, A. Schleiffer, L. Endler, G. Ammerer, *Nature* **406**, 94 (2000).
5. P. C. Hollenhorst, G. Pietz, C. A. Fox, *Genes Dev.* **15**, 2445 (2001).
6. A. Pic *et al.*, *EMBO J.* **19**, 3750 (2000).
7. P. C. Hollenhorst, M. E. Bose, M. R. Mielke, U. Muller, C. A. Fox, *Genetics* **154**, 1533 (2000).
8. R. Kumar *et al.*, *Curr. Biol.* **10**, 896 (2000).
9. K. L. Clark, E. D. Halay, E. Lai, S. K. Burley, *Nature* **364**, 412 (1993).
10. L. A. Cirillo *et al.*, *EMBO J.* **17**, 244 (1998).
11. Materials and Methods are available as supporting online material at *Science* Online.
12. F. Exinger, F. Lacroute, *Curr. Genet.* **22**, 9 (1992).
13. R. N. Fish, C. M. Kane, *Biochem. Biophys. Acta* **1577**, 287 (2002).
14. G. A. Hartzog, T. Wada, H. Handa, F. Winston, *Genes Dev.* **12**, 357 (1998).
15. R. J. Shaw, D. Reines, *Mol. Cell. Biol.* **20**, 7427 (2000).
16. T. I. Lee *et al.*, *Science* **298**, 799 (2002).
17. G. Orphanides, D. Reinberg, *Cell* **108**, 439 (2002).
18. P. Komarnitsky, E. J. Cho, S. Buratowski, *Genes Dev.* **14**, 2452 (2000).
19. C. R. Rodriguez *et al.*, *Mol. Cell. Biol.* **20**, 104 (2000).
20. E. J. Cho, M. S. Kobor, M. Kim, J. Greenblatt, S. Buratowski, *Genes Dev.* **15**, 3319 (2001).
21. D. D. Licatalosi *et al.*, *Mol. Cell* **9**, 1101 (2002).
22. I. H. Greger, N. J. Proudfoot, *EMBO J.* **17**, 4771 (1998).
23. I. H. Greger, A. Aranda, N. J. Proudfoot, *Proc. Natl. Acad. Sci. U.S.A.* **97**, 8415 (2000).
24. M. J. Dye, N. J. Proudfoot, *Mol. Cell* **3**, 371 (1999).
25. A. P. Gasch *et al.*, *Mol. Biol. Cell.* **11**, 4241 (2000).
26. H. C. Causton *et al.*, *Mol. Biol. Cell.* **12**, 323 (2001).
27. D. K. Pokholok, N. M. Hannett, R. A. Young, *Mol. Cell* **9**, 799 (2002).
28. H. Santos-Rosa *et al.*, *Nature* **419**, 407 (2002).
29. We thank A. Nair and B. Lee for outstanding technical assistance; N. Karabetsou and J. Sherriff for sharing data; A. Akoulitchev and J. Svejstrup for gifts of antibodies; B. Daignan Fornier, B. Morgan, J. Svejstrup, F. Winston, and R. Young for yeast strains and advice; and S. Lindquist for the plasmid p6431. A.M. was supported by the Human Frontier Science Program. This work was supported by The Wellcome Trust.

Supporting Online Material

www.sciencemag.org/cgi/content/full/300/5618/492/DC1
Materials and Methods
SOM Text
Figs. S1 to S8
References

10 December 2002; accepted 24 March 2003

even large fly species (*4, 5*), setting most insects apart from other flying animals such as birds and bats. If friction dominates, a fly would be required to produce torque continuously during a saccade to overcome the viscous forces acting on its body. As the fly stops producing torque, the angular velocity declines to zero almost instantly. However, the relative importance of body inertia and friction has not been tested directly, and the time course over which flies and other insects modulate aerodynamic forces during active maneuvers remains largely unknown.

To study the aerodynamics of active flight maneuvers, we captured free-flight saccades of the fruit fly, *Drosophila melanogaster*, using infrared three-dimensional (3D) high-speed video (Fig. 1A) (*6*). Within the large arena, flies were lured toward a dark vertical cylinder laced with a drop of vinegar. Although many flies approached and landed on the target, some performed collision avoidance saccades within the intersecting fields of view of the three cameras, permitting measurement of wing and body position throughout the maneuver (Fig. 1B) (*6*). We analyzed a total of six saccades, each of which was characterized by a rapid rotation of the body about the yaw axis. In the example shown in Fig. 1C, the fly starts the saccade with a path velocity of 0.19 m s^{-1}, slows down to 0.08 m s^{-1} as it changes heading, and then accelerates forward at the end of the turn. This pattern of body motion is typical of visually elicited free-flight saccades measured previously with lower spatial and temporal resolution (*3*). The improved resolution of the 3D high-speed video indicates that, despite its small size and slow speed, the animal performed a banked turn, similar to those observed in larger fly species (*7, 8*). In the example shown in Fig. 1D, the fly generated a saccade while ascending vertically at 0.13 m s^{-1}. As indicated by the time course

[1]Institute of Neuroinformatics, University/ETH Zürich, Winterthurerstr. 190, CH-8057 Zürich, Switzerland. [2]Bioengineering and Biology, California Institute of Technology, Pasadena, CA 91125, USA.

*To whom correspondence should be addressed. E-mail: flyman@caltech.edu

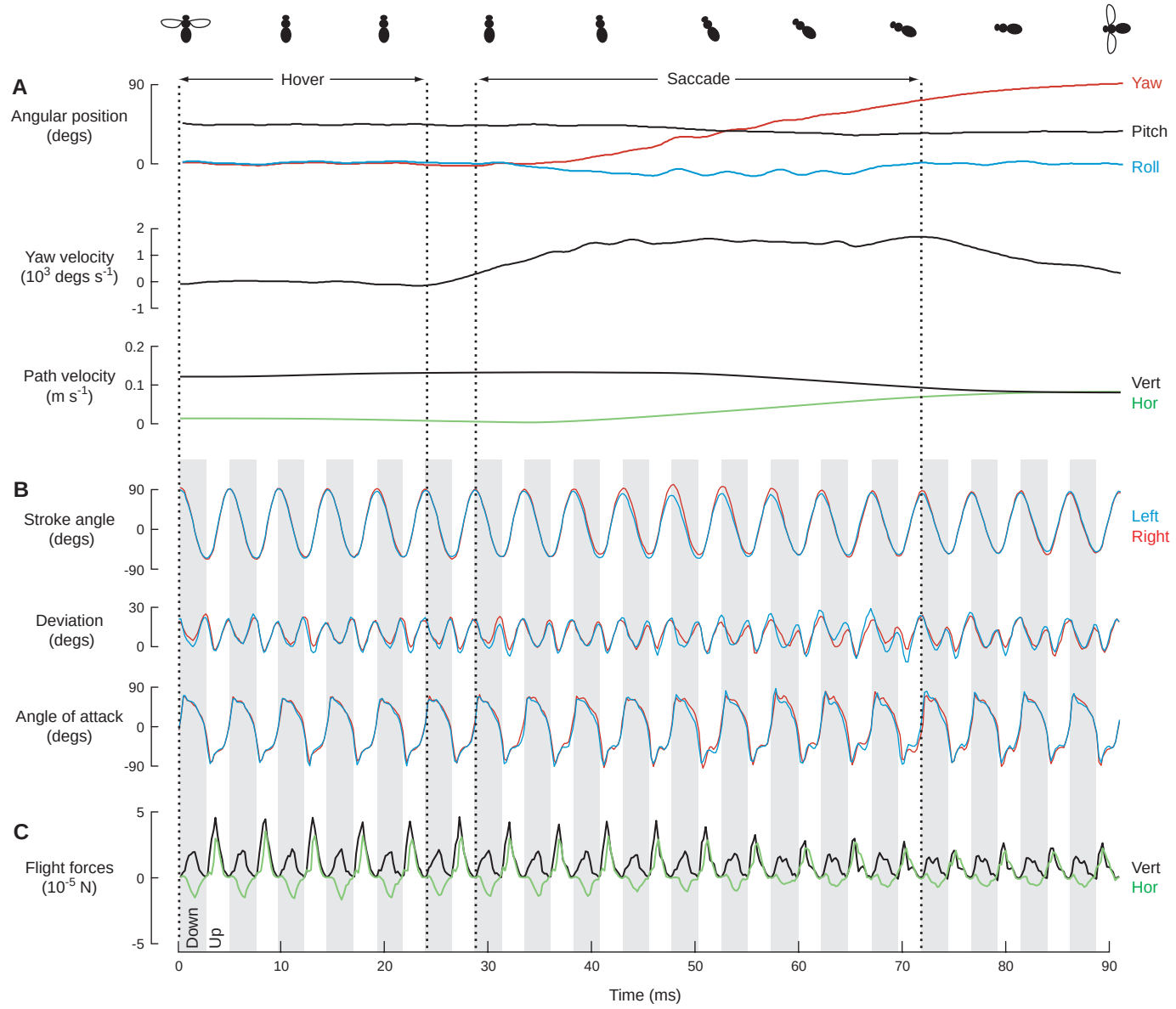

Fig. 2. Time series of flight maneuver shown in Fig. 1D. A dorsal view of the fly at the top of the figure indicates the yaw throughout the maneuver. (**A**) Yaw (red), pitch (black), and roll (blue) axis of the body. Horizontal (green) and vertical (black) path velocity are shown below. (**B**) Stroke angle, deviation, and angle of attack of the right (red) and left (blue) wing [for definitions see (*12*)]. (**C**) Horizontal (green) and vertical (black) aerodynamic forces in a fixed external reference frame.

of yaw, the animal then rotated by 90° within 50 ms, completing the maneuver within 10 wing beats.

To test whether the measured patterns of wing motion were sufficient to explain the saccades, we played the wing kinematics of all complete sequences through a dynamically scaled robotic model to measure the time-varying aerodynamic forces (Figs. 2C and 3A) (*6*). Before the onset of the saccade, the wings moved in almost perfect mirror symmetry with a nearly horizontal stroke plane and a "U-shaped" tip trajectory (Fig. 3A). For the example shown, the average vertical force throughout the stroke was 13.4 μN (Fig. 3B), which is sufficient to support the weight of a fruit fly (*6*). All of the six flies we analyzed showed similar patterns of wing motion and force production before the turn. During the saccade, the stroke kinematics changed surprisingly little from the pre-saccade pattern (Fig. 2B), indicating that rapid maneuvers are caused by quite minor changes in wing motion. Despite this small modulation of wing motion, changes in the pattern of forces are quite large during the turn (Fig. 2C). This apparent paradox is explained by the fact that the mean forces generated by a fruit fly remain relatively fixed with respect to its body axis (*9, 10*) and that changes in the horizontal and vertical force components during the saccade are due to the changing orientation of the body, just as a helicopter increases thrust by pitching downward (*11*). Thus, determining how an insect controls body attitude during a maneuver is central to the understanding of flight control.

We focused our analysis on yaw, because the fly must generate the greatest torque around this axis as a result of its elongate body shape and the 90° change in heading (Fig. 2A). To turn, the fly must generate a force moment (yaw torque) to overcome both the inertia of its body and the frictional resistance of the air's viscosity. Mathematically, this can be expressed as

$$T_\phi = I \cdot d^2\phi/dt^2 + C \cdot d\phi/dt \qquad (1)$$

where ϕ is the angular position about the yaw axis, I is the moment of inertia, C is a frictional damping coefficient, and T_ϕ is the yaw torque created by the fly. The dynamics of the saccade are determined by the ratio I/C, which represents the time constant of the system. A small time constant relative to the duration of the maneuver would imply that a fly would rapidly reach a terminal angular velocity, proportional in magnitude to the torque it creates. To stop turning, the fly would only need to cease generating torque. Conversely, if inertia dominates and the time constant is large, the fly must accelerate to start the saccade and actively decelerate to stop. Inspection of Fig. 3C shows that the time course of T_ϕ is similar to that of the fly's angular acceleration, but not its angular velocity. This suggests that $T_\phi \approx I \cdot d^2\phi/dt^2$,

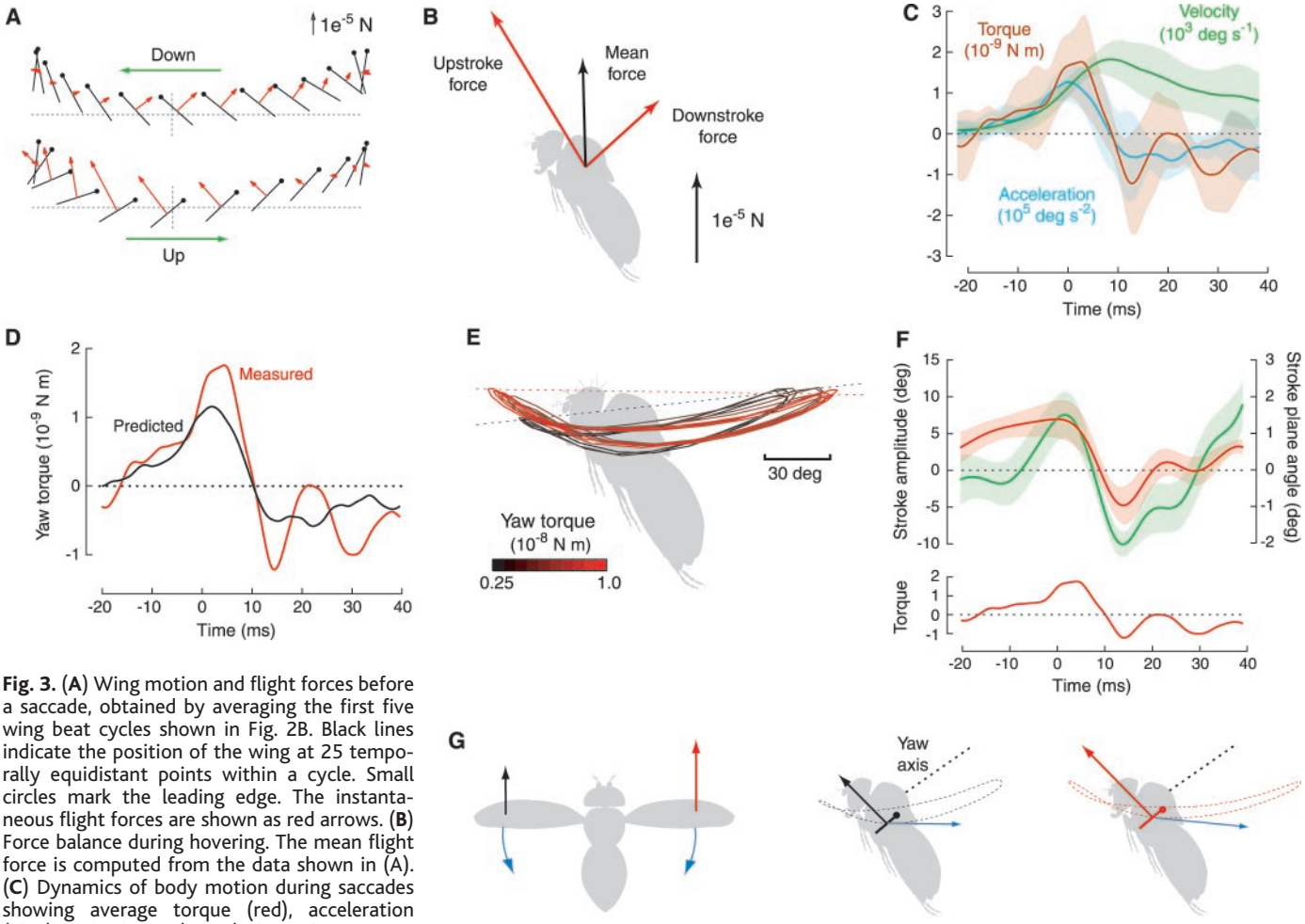

Fig. 3. (**A**) Wing motion and flight forces before a saccade, obtained by averaging the first five wing beat cycles shown in Fig. 2B. Black lines indicate the position of the wing at 25 temporally equidistant points within a cycle. Small circles mark the leading edge. The instantaneous flight forces are shown as red arrows. (**B**) Force balance during hovering. The mean flight force is computed from the data shown in (A). (**C**) Dynamics of body motion during saccades showing average torque (red), acceleration (blue), and velocity (green) about the yaw axis ($N = 6$, shaded areas denote ±1 SD). The flight samples were aligned in time with respect to the local torque maximum, denoted zero on the abscissa. (**D**) Comparison of measured torque (red) with values estimated from body motion and morphology (black). (**E**) Relationship between changes in the wing tip trajectory and yaw torque produced by a wing. (**F**) Difference in stroke amplitude (red) and stroke plane angle (green) between the outside and the inside wing during saccades ($N = 6$, shaded areas denote ±1/4 SD). Average torque from (C) is plotted below for comparison. (**G**) Aerodynamic basis of yaw control. To initiate a turn to the left, the fly creates a torque by increasing the stroke amplitude on the outside wing (raising velocity) as well as by tilting the stroke plane backward (increasing the aerodynamic angle of attack).

indicating that the dynamics of the small fly are dominated by body inertia and not friction.

This assertion was further tested in several ways. First, we calculated I and C on the basis of the animal's body morphology (*6*). The values ($I = 5.2 \times 10^{-13}$ N m s^2, $C = 5.2 \times 10^{-13}$ N m s) yield a time constant $\tau = I/C = 1$ s, about 20 times the duration of a single saccade. Second, we replayed the measured wing kinematics during the saccades through the robot to generate a time course of yaw torque, T_ϕ, throughout the maneuver. We then derived I and C from a multilinear regression of T_ϕ on the measured body kinematics (*6*). This procedure yielded a value of $5.9 \times 10^{-13} \pm 3.3 \times 10^{-14}$ N m s^2 for I, and a value of $1.1 \times 10^{-12} \pm 2.3 \times 10^{-11}$ N m s for C (mean $\pm$ SD, $N = 6$). The corresponding time constant, 0.53 s, although smaller than that derived from body morphology, is still 10 times the duration of a saccade. Finally, we calculated the torque required to generate the observed body kinematics according to Eq. 1, using the morphologically based values of I and C. Given the assumptions and potential sources of error in our analysis, the time course of the predicted torque based solely on body motion and morphology matches well the time course of torque measured independently by playing the wing kinematics through the robot (Fig. 3D). It is not surprising that the torque estimated from body kinematics underestimates that measured from wing motion. The calculated value of C is most likely an overestimate because it is based on Stokes' Law and assumes a very low Reynolds number for the rotation, whereas the calculation of I is likely an underestimate because added mass effects have been ignored. Collectively, the results strongly contradict previous assumptions that the flight dynamics of flies are dominated by friction (*4, 5*).

To determine how flies change wing motion to generate yaw torque, we sorted all stroke cycles within the entire data set according to the magnitude of yaw torque created during each cycle (Fig. 3E). Two specific changes in wing motion correlate most strongly with measured yaw torque: a backward tilt of the stroke plane and an increase in stroke amplitude (Fig. 3, E and F). The backward tilt of the stroke plane accompanies an increase in the aerodynamic angle of attack that elevates flight force during the upstroke. This augmentation at the start of the upstroke has a particularly potent effect on yaw torque because the force created by the wing is roughly orthogonal to the fly's yaw axis at this point in the cycle (Fig. 3, A, B, and G). The change in torque is further augmented by an increase in stroke amplitude, which elevates wing velocity (Fig. 3G). Other parameters, such as subtle changes in angle of attack relative to the stroke path (Fig. 2B), may also play a role. At the onset of a saccade, the outside wing tilts back and beats with a greater stroke amplitude relative to the inside wing (Fig. 3F). After 12.5 ms, the conditions reverse, in accordance with the need to generate countertorque to decelerate.

These experiments show how tiny insects control aerodynamic forces to actively maneuver through their environment. Although the analyses rely on several simplifying assumptions (*6*), these are not critical for the main conclusions drawn. The internal consistency of the data further corroborates that the measurements were performed with adequate precision. The results indicate that even in small insects the torques created by the wings act primarily to overcome inertia, not friction. Because of the minor importance of frictional coupling, a countertorque is necessary to terminate the rotation of the body. The torques required to turn are produced by remarkably subtle changes in wing motion. A slight tilt of the stroke plane angle and a minor change in stroke amplitude are sufficient to accelerate the animal around the yaw axis. Although these experiments were performed on tiny fruit flies, the results are relevant for nearly all insects, because the relative importance of rotational inertia over friction increases with size. Collectively, these results provide an important basis for future research on the neural and mechanical basis of insect flight, as well as insights for the design of biomimetic flying devices.

References and Notes

1. T. S. Collett, M. F. Land, *J. Comp. Physiol.* **99**, 1 (1975).
2. C. Schilstra, J. H. van Hateren, *J. Exp. Biol.* **202**, 1481 (1999).
3. L. F. Tammero, M. H. Dickinson, *J. Exp. Biol.* **205**, 327 (2002).
4. W. Reichardt, *Naturwissenschaften* **60**, 122 (1973).
5. _____, T. Poggio, *Q. Rev. Biophys.* **9**, 311 (1976).
6. See supporting data on *Science* Online.
7. H. Wagner, *Philos. Trans. R. Soc. London Ser. B* **312**, 527 (1986).
8. C. Schilstra, J. H. van Hateren, *Nature* **395**, 654 (1998).
9. S. Vogel, *J. Exp. Biol.* **44**, 567 (1966).
10. K. G. Götz, *Kybernetik* **4**, 199 (1968).
11. C. T. David, *Physiol. Entomol.* **3**, 191 (1978).
12. S. P. Sane, M. H. Dickinson, *J. Exp. Biol.* **204**, 2607 (2001).

13. We thank J. Birch, W. Dickson, S. P. Sane, and J. Staunton for technical advice and assistance. S.N.F. thanks D. Robert for scientific advice and I. Fry-Berg for personal support. Supported by grants from NSF and the Packard Foundation (M.H.D.) and by the Swiss National Science Foundation (S.N.F.).

Supporting Online Material

www.sciencemag.org/cgi/content/full/300/5618/495/DC1
Materials and Methods
References
Movie S1

27 December 2002; accepted 21 March 2003

Environmental Noise Retards Auditory Cortical Development

Edward F. Chang* and Michael M. Merzenich

The mammalian auditory cortex normally undergoes rapid and progressive functional maturation. Here we show that rearing infant rat pups in continuous, moderate-level noise delayed the emergence of adultlike topographic representational order and the refinement of response selectivity in the primary auditory cortex (A1) long beyond normal developmental benchmarks. When those noise-reared adult rats were subsequently exposed to a pulsed pure-tone stimulus, A1 rapidly reorganized, demonstrating that exposure-driven plasticity characteristic of the critical period was still ongoing. These results demonstrate that A1 organization is shaped by a young animal's exposure to salient, structured acoustic inputs—and implicate noise as a risk factor for abnormal child development.

Soon after the onset of hearing in the rat (postnatal day 12, or P12), a large auditory cortical area dominated by broadly tuned, high-frequency–selective neurons can be defined in the temporal cortex (*1*). Through a subsequent ~2- to 3-week critical period, the infant rat's auditory cortex undergoes extensive refinement to acquire an adultlike organization. Adult rats exhibit a compact, tonotopically ordered "primary auditory cortex" (A1) that represents the full spectrum of acoustic inputs with sound frequency–selective neural responses (*1*, *2*). A1 organization is easily distorted within this early postnatal period by exposure to specific acoustic inputs, indicating that the normal development of the auditory cortex is substantially influenced (and potentially strongly biased) by the structure of environmental acoustic inputs in early life (*1*, *3*). In the human infant, the emergent selective representation of the pho-

W. M. Keck Center for Integrative Neuroscience, University of California, San Francisco, CA, USA.

*To whom correspondence should be addressed. E-mail: echang@itsa.ucsf.edu